SERBIAN JOURNAL OF ELECTRICAL ENGINEERING
Vol. 21, No. 3, October 2024, 407-428
UDC: 621.397:004.93 **DOI: https://doi.org/10.2298/SJEE2403407I**

A Novel Super Frame Flexible Macroblock Ordering Scheme for H.265 Video Transmission with Unequal Error Protection

Deevya Indoonundon[1], Tulsi Pawan Fowdur[1], Sunjiv Soyjaudah[1]

Abstract: One of the most popular video coding standards in use today is High Efficiency Video Coding (HEVC), also known as H.265. In this paper, a novel Flexible Macroblock Ordering (FMO) scheme known as Super frame FMO (SFMO) is proposed for HEVC video compression. The SFMO scheme is combined with a concealment aware Unequal Error Protection (UEP) scheme using RS codes and interleaved to improve the performance of the RS decoder. Moreover, Multiple Description Coding (MDC) is used to further improve its performance. The simulation results have shown that the proposed system surpassed an Equal Error Protection (EEP) scheme by an average gain of 3.02 dB in the range of $0.1 \leq$ Packet Loss Rate ≤ 0.5 with FLI (Frame Level Interleaving)-SFMO. Additionally, the FLI- SFMO scheme outperformed Explicit Chessboard-Wipe (ECW) FMO by an average gain of 1.48 dB.

Keywords: High Efficiency Video Coding, Super frame Flexible Macroblock Ordering, Multiple Description Coding, Unequal Error Protection.

1 Introduction

Over the past ten years, there has been an increase in bandwidth demand due to the adoption and integration of advanced digital technology [1]. According to the most recent report by the Ericsson group [2], video traffic currently makes up 69% of all mobile data traffic and is projected to increase to 79% in 2027. Video compression, which significantly reduces the size of the video file, is a popular way to lower the bandwidth requirement for video transmission. Numerous studies have been done in the field of video compression for a long time. HEVC, which is one of the most popular video compression methods, has gained awareness on a global scale [3]. HEVC has demonstrated up to a 50% compression ratio compared to H.264, its predecessor [4] and the effectiveness of HEVC has been demonstrated in several recent studies [5 – 8]. However, transmitting compressed video via unstable communication channels is extremely

[1]University of Mauritius, Department of Electrical and Electronic Engineering, Reduit, Mauritius;
Emails: deevya.indoonundon1@umail.uom.ac.mu, p.fowdur@uom.ac.mu, sunjivsoyjaudah@gmail.com

difficult because even a single packet loss can cause the video to completely degrade. Therefore, the usage of error-correcting techniques is essential to ensure that the video is received effectively. Reed Solomon codes have become one of the most used methods for correcting packet loss errors over time [9]. The HEVC encoded data can be enhanced with RS codes to include redundant information that enables error correction when transmitted over noisy channels. Additionally, the RS encoded array can use interleaving to improve error correction [10]. A successful and extensively used error-resistant strategy is Flexible Macroblock Ordering [11]. To prevent the transmission of consecutive Macroblocks (MBs), FMO reorders the MBs transmission order [11]. An interesting approach is to use Unequal Error Protection to provide more protection to important MBs to ensure effective concealment in case the latter could not be corrected by the RS decoder [10]. An additional strategy is to combine FMO with Interleaving methods before transmission to improve the RS decoder's ability to repair errors. In addition, packet losses can be avoided by using Multiple Description Coding [12].

FMO is one of the most popular error resilient tools which has been extensively used to enhance video transmission. For instance, the author of [13] proposed an efficient and adaptive hybrid error resilience and error correction method for 3DV transmission that utilised slice structured coding, context adaptive variable length coding, and FMO. The suggested error resilient system has demonstrated to deliver up to 2.85 dB gain at high packet loss rates of 0.4 when used in conjunction with existing error correcting techniques. Additionally, in [14], a unique video encryption strategy based on FMO scrambling was suggested, and the experimental findings have demonstrated that the proposed scheme could secure the scrambled video with a small computational overhead. A new FMO technique based on an enhanced three-dimensional flexible macroblock ordering was also presented by the authors in [15]. (3D FMO). According to the findings, an IP-based broadcast video application can achieve a gain of 1-2 dB with a 10% packet loss.

Forward Error Correction (FEC) is a technique which allows for the detection and correction of a small number of faults in transmitted data without the need for retransmission [16]. Unequal error protection (UEP) is used to provide asymmetric protection for messages with various levels of priority to reduce the energy wasted in communications [17]. In decoding-and-forward (DF) relay systems, the researchers in [17] suggest novel effective UEP techniques based on bilayer protograph-based low-density parity check (PLDPC) codes. In addition, to create UEP techniques and subsequently conserve transmission energy, source coding and channel coding were utilized. The simulation results demonstrate that the suggested UEP schemes significantly outperform the traditional equal error prevention (EEP) scheme in terms of performance [17]. In [18], a novel UEP rateless code is presented that uses a duplication method and a shift operation in the zigzag decodable fountain codes. It is demonstrated that the

suggested code can enhance the symbol recovery rate of input symbols with high priority levels while barely degrading the performance of other input symbols. Furthermore, in [19] the advantages and disadvantages of various forward error-correction (FEC) codes, such as turbo, LDPC, convolutional, RS, polar, and BCH were investigated. The comparison showed that even while LDPC codes offer a substantial capacity for error correction, the error floor phenomenon limits their employment in applications where error rates need to be reduced. In contrast to other coding techniques, the performance of polar codes was seen to be essential in finite-length regimes. RS and BCH codes, as opposed to convolutional and turbo codes, had greatly improved system performance and simple decoding, making them the best forward error-correction codes for LTE systems. However, RS codes surpassed BCH codes in terms of BER performance because of their large error-correcting capacity.

In this paper, a novel Super Frame FMO (SFMO) scheme is proposed and used in conjunction with a recently developed UEP scheme for HEVC using RS Codes [10] and MDC. The new SFMO scheme is based on the concept where all the frames within a GOP are re-arranged to form a super-frame structure. In addition, the SFMO model is used with two types of interleaving techniques presented in [10] referred as, Frame Level Interleaving (FLI) and Group Level Interleaving (GLI). This paper therefore introduces two new FMO schemes referred to as FLI-SFMO and GLI-SFMO which adapt to each type of interleaving, FLI and GLI, to further improve the performance of the RS decoder. In addition, the system was combined with MDC to minimize the effect of channel errors. With MDC two different loss models namely, the Gilbert Elliot channel and the composite channel model were simulated. The simulation results have shown that the proposed system surpassed an EEP scheme by an average gain of 3.02 dB in the range of $0.1 \leq PLR \leq 0.5$ with FLI-SFMO. Moreover, the FLI-SFMO scheme outperformed ECW-FMO by an average gain of 1.48 dB for an MDC transmission using Gilbert Elliot channel model.

The main contributions of the paper are as follows:

1. Development of a novel Flexible Macroblock Ordering scheme for HEVC known as the Super Frame FMO with two different interleaving schemes namely frame level and group level interleaving.
2. Incorporation of UEP and MDC in the proposed SFMO scheme to increase its resilience to channel errors.
3. Performance analysis of the proposed scheme using two channel models and comparison with conventional FMO schemes.

The remainder of this paper is organized as follows. Section 2 presents the research method of the proposed framework. Section 3 demonstrates the experimental results and finally, Section 4 draws some conclusions and scope for future works.

2 System Model

The proposed encoder is shown in Fig. 1.

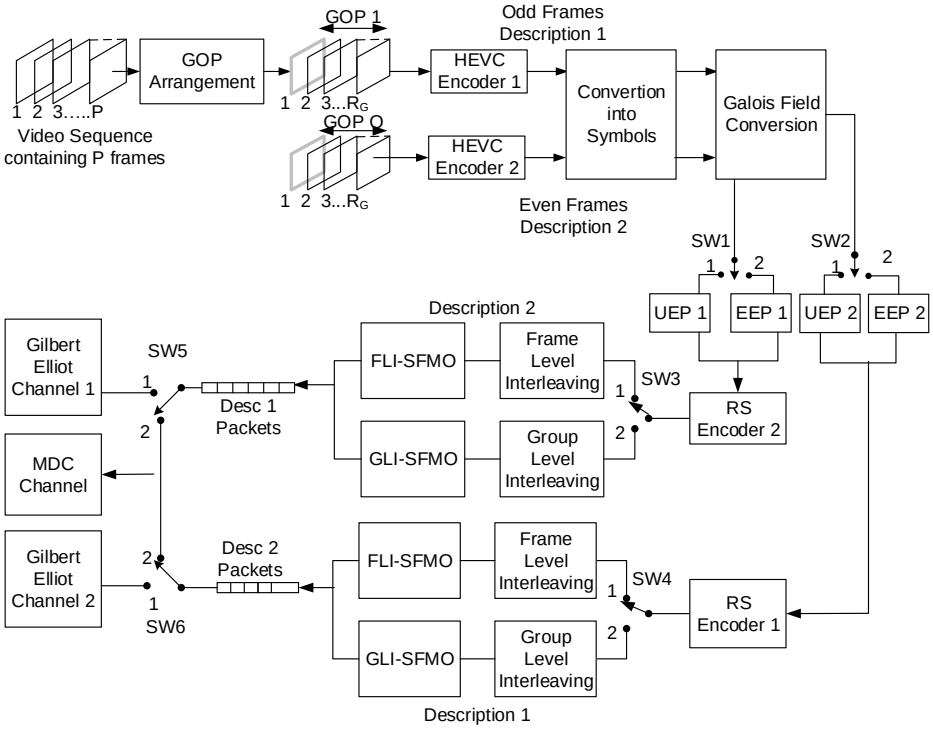

Fig. 1 – *Proposed Encoder*.

The input to the encoder consists of Q, Group of Pictures each of which has a length of RG, generating a video sequence of length, P such that:

$$P = R_G \times Q\,, \tag{1}$$

where P represents the length of the video sequence, R_G represents the length of each GOP, and Q represents the number of GOPs.

The proposed system's encoder is shown in Fig. 1. A novel FMO scheme is proposed which transmits the packets in such an order which greatly enhances the error correcting capability of the RS decoder. The new FMO scheme is applied to an existing RS encoding scheme as described in [10]. Each FMO scheme is adapted to the type of interleaving scheme used. For instance, FLI-SFMO scheme is used for the FLI whereas GLI-SFMO is used for the GLI. Moreover, this paper also proposes a novel combination of an existing MDC scheme as described in [12] with the new FMO Scheme.

The MBs are processed separately by two HEVC encoders, Encoder 1 and Encoder 2 to form two different arrays of bits each representing a description, description 1 and description 2 respectively. After the encoding process, description 1 consists of odd numbered frames whereas description 2 consists of even numbered frames. The array of bits is then converted into symbols to enable Galois field conversion. After the transformation into Galois field arrays, either EEP or UEP is used to assign different protection levels for the MBs in each description. For UEP to take place switches SW1 and SW2 are placed in position 1.

To select EEP, switches SW1 and SW2 are placed in position 2. EEP1 and EEP2 represents the same EEP rate which has been applied to each description, description 1 and description 2 respectively. RS encoding then takes place where each array of symbols of length, L_s is then converted into k symbols by the RS encoder using a bit rate, R_b, as follows:

$$L_s = k \times R_b , \tag{2}$$

Two types of interleaving as described in [10] are used namely FLI and GLI. To select FLI, switches SW3 and SW4 are placed in position 1. For GLI selection, SW3 and SW4 are placed in position 2. The new FMO scheme is then adapted to the type of interleaving technique to enhance the performance of the RS encoder. Further details on the interleaving schemes are given in Section 2.1. The output of the encoder are two different packet arrays each representing a description. The type of MDC channel is then selected by either using the Gilbert Elliot channel model or the composite channel model. For Gilbert Elliot channel selection, SW5 and SW6 are placed in position 1 and for the composite channel model SW5 and SW6 are placed in position 2.

Fig. 2 illustrates the proposed decoder. The packets of both description 1 and description 2 are received at the input of the decoder following the transmission over either the composite or the Gilbert Elliot channel model. Next, inverse SFMO is applied to the packets of each description so as to rearrange the MBs in their original positions before de-interleaving is performed. For using Inverse FLI-SFMO and FLI De-Interleaving, SW7 and SW8 are placed in position 1. Otherwise, if Inverse GLI-SFMO and GLI De-Interleaving are to be performed, SW7 and SW8 are placed in position 2. If the UEP scheme is used, SW9 and SW10 are placed in position 1 and for the EEP scheme, SW9 and SW10 are placed in position 2. Error correction is then performed on the packets of each description with the use of RS Encoding. The RS decoder outputs arrays of symbols for each description after each symbol to bits conversion is performed. The HEVC decoders then transform the bits into frames following which both descriptions are merged to form one Video sequence. Finally, prioritised concealment [20] is performed.

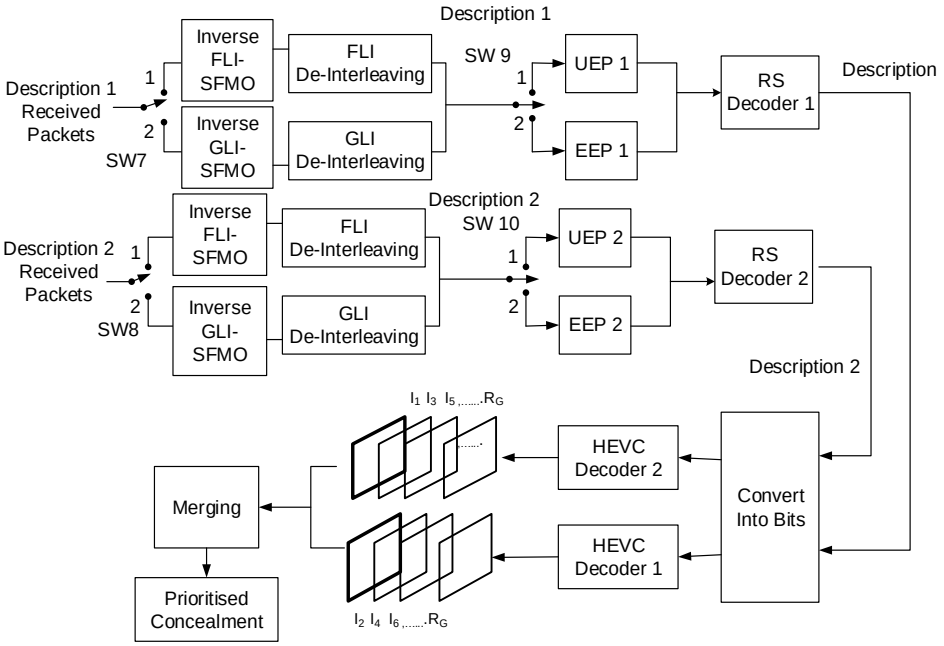

Fig. 2 – *Proposed Decoder.*

2.1 Proposed SFMO scheme

In this paper, a new SFMO technique has been developed to re-arrange the MBs to enhance the performance of the RS Encoder. From [10], it was observed that with the use of UEP, greater error correcting capability can be achieved. The error correcting capability of an RS encoder is given by the equation below:

$$E_t = \frac{n_s - k_s}{2}, \tag{3}$$

where k_s represents the length of the symbol array of each MB and n_s represents the length of the codeword after the addition of $n_s - k_s$ parity symbols.

Another method to enhance the performance of the RS encoder is to rearrange the MBs in such an order to distribute the burst errors throughout the video sequence thereby ensuring that the total number of packet errors, N_E, is less that E_t, the error correcting capability of the RS encoder. This methodology ensures a perfect reconstruction of the video sequence. For each interleaving scheme, a FMO scheme has been designed to ensure that N_E does not exceed E_t. A description of each FMO scheme is given in Section 2.1.1 and 2.1.2.

2.1.1 FLI – SFMO

Fig. 3 illustrates the FLI- SFMO process. First, FLI is performed where packets are formed by merging symbols from each of the 99 MBs of each of the frames F_1, F_2, F_3, F_4 and F_5 [10]. The idea is to propagate the information pertaining to an MB so that the RS encoder can correct the errors at high packet losses. The number of symbols N_f required from each MB to form a packet is given by equation as follows [10]:

$$N_f = n_s/99, \tag{4}$$

where n_s represents the length of the codeword.

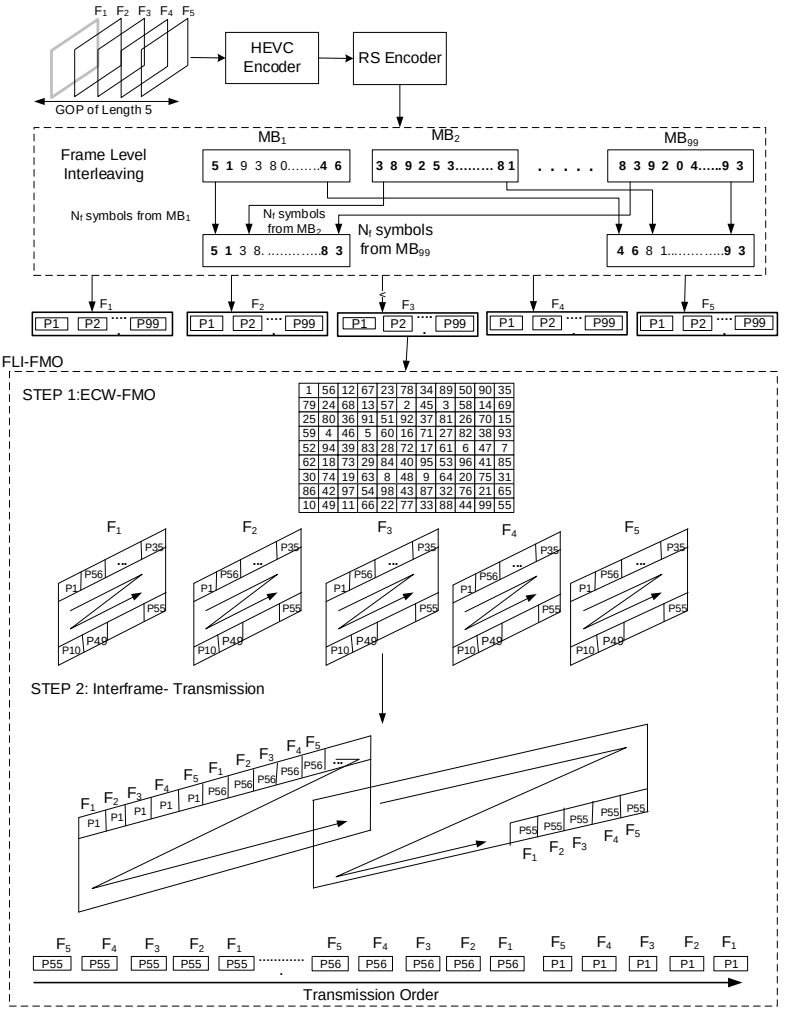

Fig. 3 – *Illustration of FLI-SFMO with FLI.*

Fig. 3 illustrates how N_f symbols from each MB, MB_1, MB_2 up to MB_{99} are merged to form the first packet. For example, MB_1 which is made up of symbols 5,1,9,3,8,0 up to 6, is interleaved by taking N_f symbols from each MB. This process is repeated until 99 packets are formed from all the frames within a GOP.

Following the Interleaving process, the novel FLI-SFMO scheme is applied. This process consists of two steps. Firstly, ECW- FMO [11] is applied where the packets are transmitted in the ECW -FMO order of transmission. Fig. 3 shows the frames after ECW- FMO [11] has been performed. Secondly, interframe transmission is performed such that packet P1 from Frame 1, F_1, is transmitted followed by P1 from frame F_2 and so on. This further propagates the frames such that the distance between two consecutive packets is increased further.

2.1.2 The Selection Algorithm with FLI-SFMO

Fig. 4 represents the FLI-SFMO algorithm.

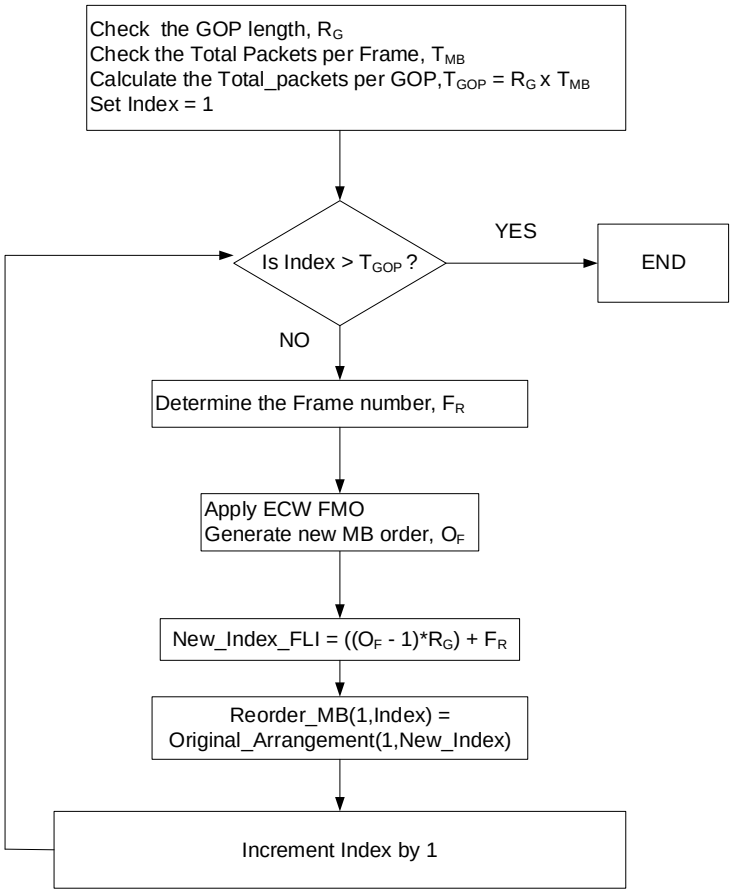

Fig. 4 – *Flowchart representing the selection process.*

First the algorithm computes the total number of MBs in a GOP by using the (5) as follows:

$$T_{GOP} = R_G \times T_{MB}, \tag{5}$$

where T_{GOP} refers to the total number of MBs in a GOP, R_G refers to the total number of frames in a GOP and T_{MB} refers to the total number of MBs in a frame.

The index is set to 1 and the transmission order of each MB will be determined by assigning a new index to it. The frame number, F_R, to which each MB belongs is first determined. Then, the algorithm checks the type of interleaving which was used.

If FLI interleaving is used, ECW FMO [11] is first applied to reshuffle the MBs in a frame and a new packet order, $O_{F,}$ is assigned to each MB. After ECW FMO, interframe rearrangement is performed as per the below equation:

$$New_{Index_{FLI}} = ((O_F - 1) * R_G) + F_R, \tag{6}$$

Where O_F refers to the new packet order after ECW-FMO, R_G refers to the GOP length and F_R refers to the frame number within a GOP.

2.1.3 Loss Scenario with FLI-SFMO

Consider a loss scenario where burst errors occur during transmission of packets 9, 10 and 11 of the second frame, F_2 as shown in Fig. 5. Since the burst errors are consecutive and occurred during the transmission of the same frame F_2, it will be challenging to correct the errors. After application of ECW-FMO [11], the transmission order has changed where packets 9, 10 and 11 have been replaced by packets 50, 90 and 35 respectively. After conducting the interframe shuffling as per (6), a new transmission order has been assigned as follows (R_G, GOP length = 5; F_R, Frame number = 2):

If O_F = 50

$$New_{Index_{FLI}} = ((50-1)*5) + 2 = 247.$$

If O_F = 90

$$New_{Index_{FLI}} = ((90-1)*5) + 2 = 447.$$

If O_F = 35

$$New_{Index_{FLI}} = ((35-1)*5) + 2 = 172.$$

This method has greatly increased the distance between the transmission of two erroneous packets. As seen in Fig. 5, each erroneous frame is located in different frames which ensures that the latter will be corrected by the RS encoder.

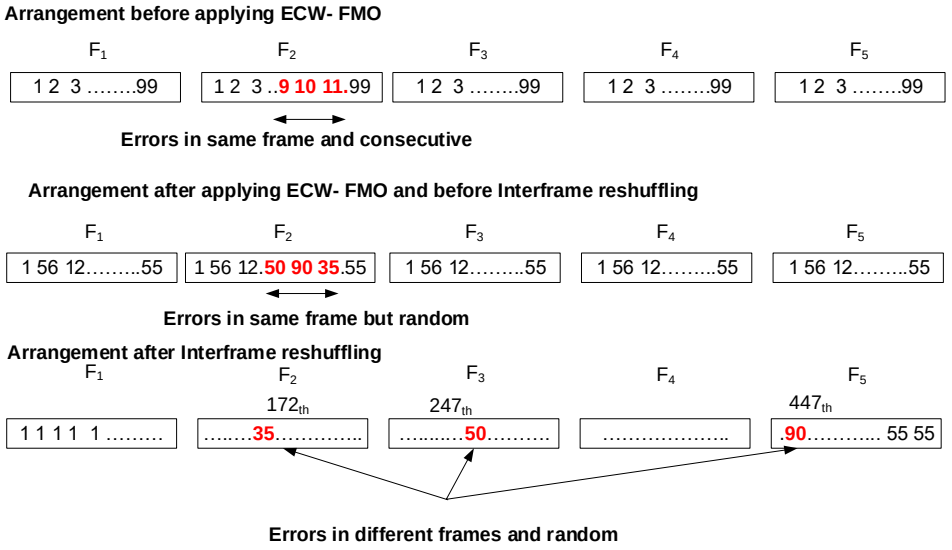

Fig. 5 – *Loss Scenario with FLI-SFMO.*

2.1.4 GLI- SFMO

Fig. 6 illustrates the GLI-SFMO scheme.

First, GLI [10] is applied where the MBs are assembled to form 9 slices after which interleaving is performed across each slice consisting of 11 MBs.

$$N_f = n_s / 11, \tag{7}$$

As compared to the previous scheme, Type 5 FMO is used so as to separate the MBs belonging to a same slice. Type 5 FMO first distributes the packets in such a way that no consecutive packets belong to the same slice. After Type 5 FMO, interframe transmission is applied.

2.1.5 The Selection Algorithm with GLI-SFMO

If GLI Interleaving is used, Type 5-FMO is applied and a new index, O_G is allocated to each MB. Lastly, interframe rearrangement is performed by using the following equation:

$$New_{Index_{GLI}} = ((O_G - 1) * R_G) + F_R, \tag{8}$$

where O_G refers to the new packet order after Type 5-FMO.

The process is repeated until all the MBs have been assigned a new order of transmission.

Fig. 7 represents the GLI-SFMO algorithm.

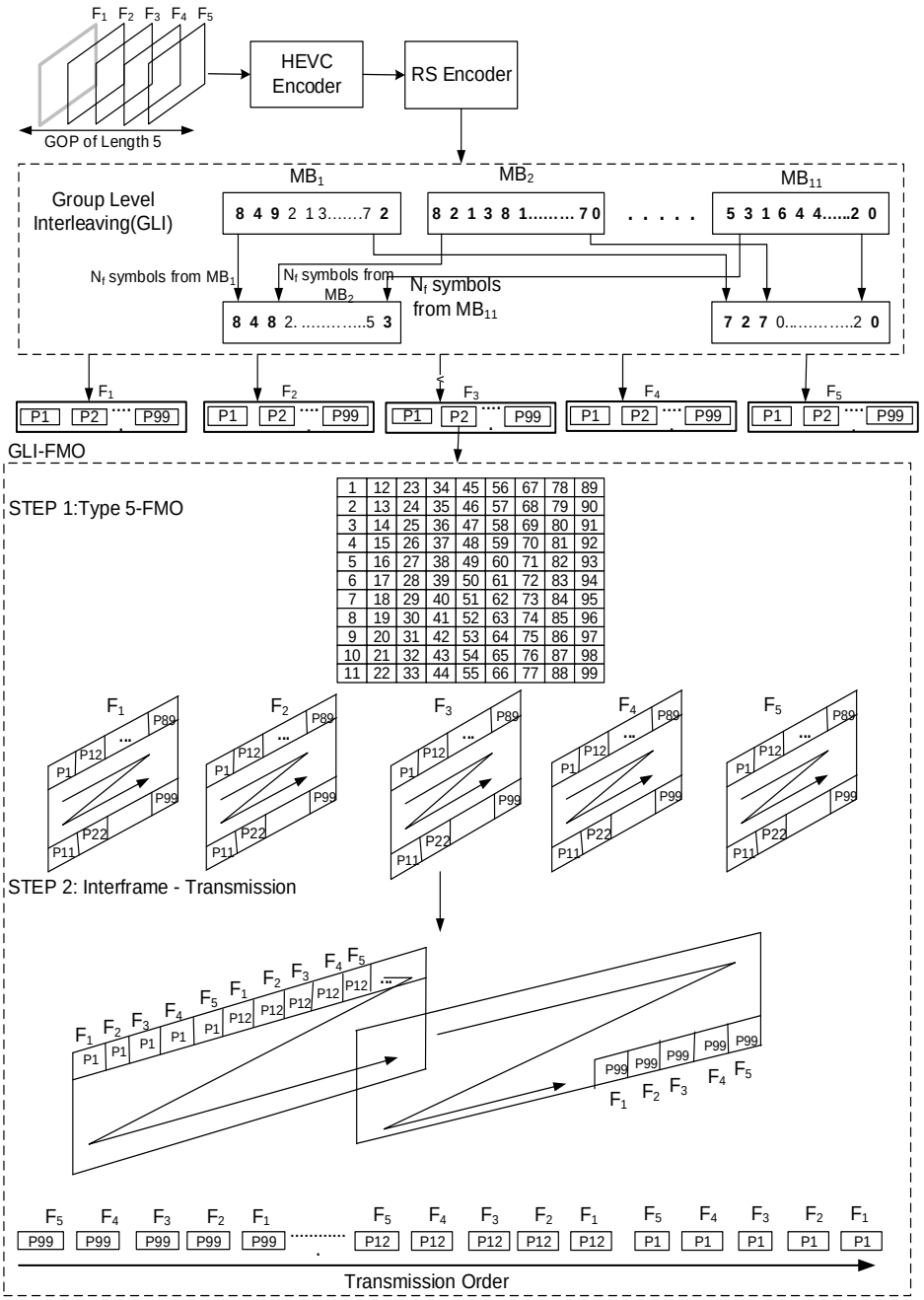

Fig. 6 – *Illustration of GLI-SFMO with GLI.*

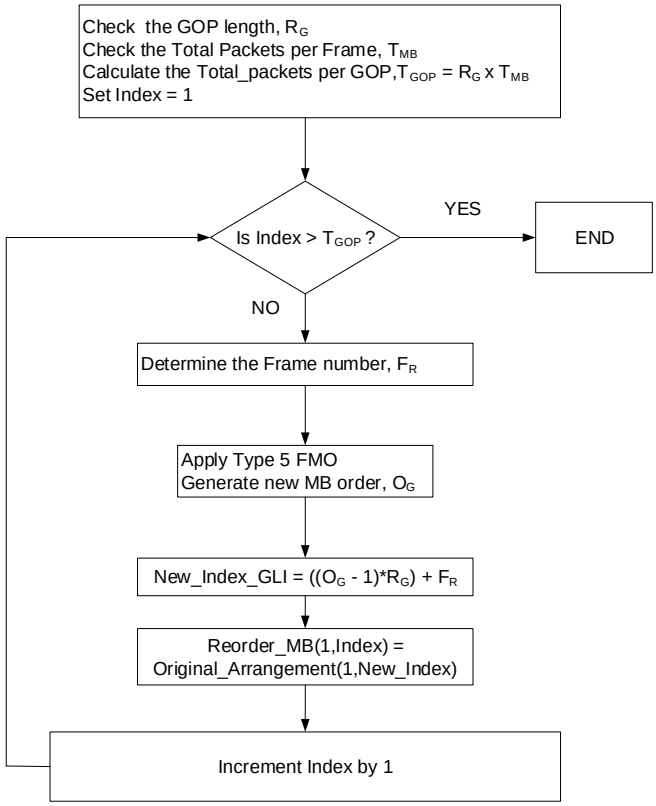

Fig. 7 – *Flowchart representing the selection process.*

2.1.6 Loss Scenario with GLI-SFMO

Consider a loss scenario where the same burst errors as in Section 2.1.4 as shown in Fig. 8. With GLI-SFMO, Type 5-FMO is used where the transmission order of packets 9, 10 and 11 has been replaced by packets 89, 2 and 13 respectively. After conducting the interframe shuffling as per (8), a new transmission order has been assigned as follows (R_G, GOP length = 5; F_R, Frame number = 2):

If $O_G = 89$

$$New_{Index_{GLI}} = ((89-1)*5)+2 = 442 .$$

If $O_G = 2$

$$New_{Index_{GLI}} = ((2-1)*5)+2 = 7 .$$

If $O_G = 13$

$$New_{Index_{GLI}} = ((13-1)*5)+2 = 62 .$$

This method has greatly increased the distance between the transmission of two erroneous packets. With this method, two erroneous packets 2 and 13, are located within a same frame F_1, but are situated in two different slices which allows the RS encoder to correct the errors since with GLI-SFMO error correction is performed at slice level.

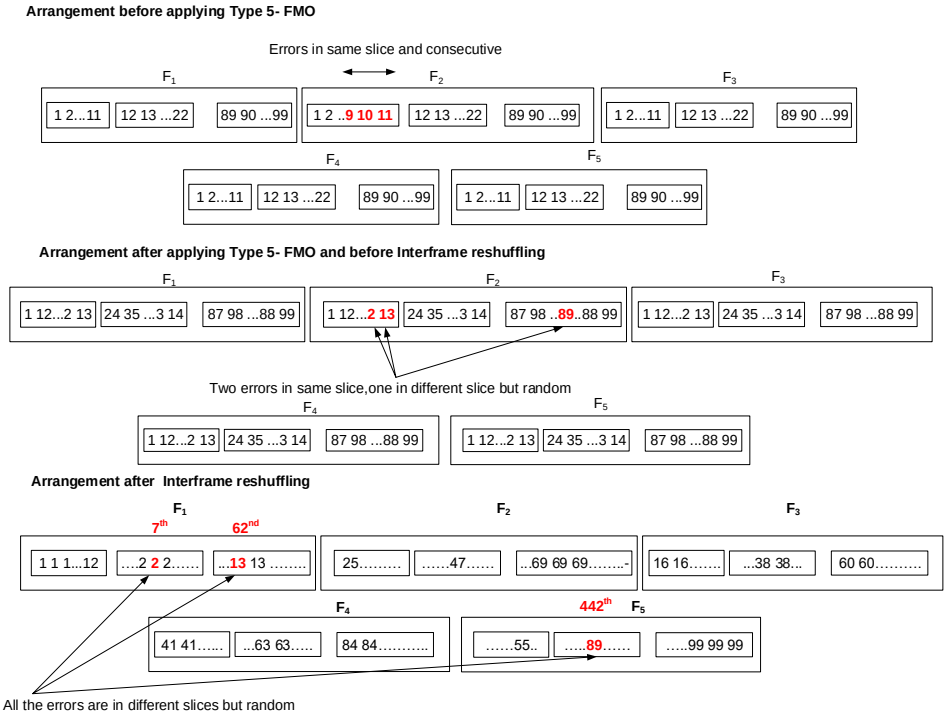

Fig. 8 – *Loss Scenario with GLI-SFMO.*

3 Simulation Results and Analysis

To assess the performance of the proposed system, five schemes have been compared. The schemes have been simulated using Matlab software using the parameters given in **Table 1**.

Table 1

List of Parameters.

Video Sequence	Foreman Sequence
Framerate	25 frames per second
Frame Size	144x176
Number of frames	300
GOP Length	5
Channel Model	Gilbert Elliot Model, Composite Channel Model

In [10], all the schemes were simulated using Single description coding and without the use of the novel FMO scheme. For instance, in this work the performance of five schemes have been analysed. In **Table 2**, a brief summary of the schemes is given. Scheme 1 represents the conventional scheme where EEP is used without a FMO scheme. Scheme 2 uses EEP and ECW-FMO [11] whereas Scheme 3 uses EEP with either GLI-SFMO and FLI-SFMO based on the type of interleaving utilized. Scheme 4 uses UEP and ECW-FMO [11] whereas Scheme 5 uses UEP with either GLI-SFMO or FLI-SFMO. In all the schemes prioritized concealment has been used as described in [20]. In addition, Concealment Dependent Index (CDI) as proposed in [10] is used such that a different rate is allocated to each packet based on firstly their location in a Frame, either border or Middle and secondly the type of frame, either I-Frame or P-Frame [10]. The rate allocation for the UEP and EEP schemes are given in **Table 3**.

Table 2
Schemes Tested.

Schemes	Rate Allocation		FMO Type	
	UEP	EEP	GLI-SFMO/FLI-SFMO	ECW-FMO [16]
1	No	Yes	No	No
2	No	Yes	No	Yes
3	No	Yes	Yes	No
4	Yes	No	No	Yes
5	Yes	No	Yes	No

Table 3
Rate Allocation for the UEP and EEP Schemes.

		Rate Allocation	
		UEP	EEP
I Frame	CDI < 8	1/4	7/20
	CDI = 8	1/3	7/20
P Frame	CDI < 4	1/3	7/20
	CDI = 4	2/5	7/20

3.1 Results using SDC with FLI-SFMO and GLI-SFMO

Fig. 9 illustrates a graph of Y-PSNR (dB) against Packet Loss Rate (PLR) with a GOP length of 5 and FLI. Scheme 5 which uses FLI-SFMO surpasses Scheme 4 where ECW-FMO [11] is used by an average gain of 1.1 dB. With FLI-SFMO, the inter-frame distribution of the packets causes the erroneous packets to be re-arranged in separate frames which allow the RS decoder to correct the errors. However, with ECW-FMO, the erroneous packets are located within the same frame which is beyond the error-correcting capability of the RS decoder. In addition, Scheme 5 which uses UEP outperforms Scheme 3 which uses EEP by

an average gain of 3.50 dB in the range of $0.1 \leq PLR \leq 0.5$. With the use of UEP, more protection is allocated to most important packets based on their CDI value. Therefore, in case the RS decoder is unable to correct an error, UEP allows an effective concealment for recovering the corrupted MBs.

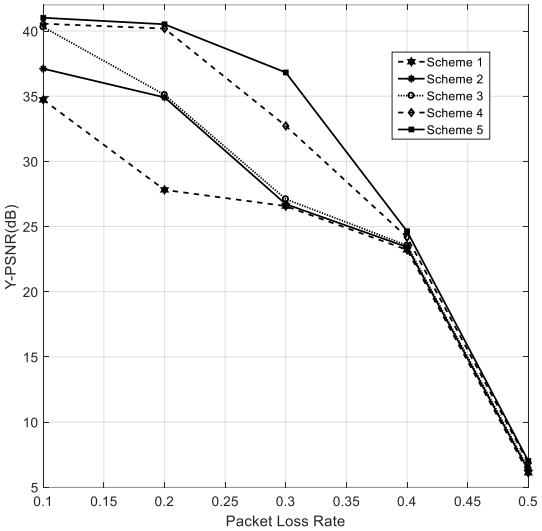

Fig. 9 – *Graph of Y-PSNR (dB) against Packet Loss Rate using SDC with FLI with the Foreman Video Sequence.*

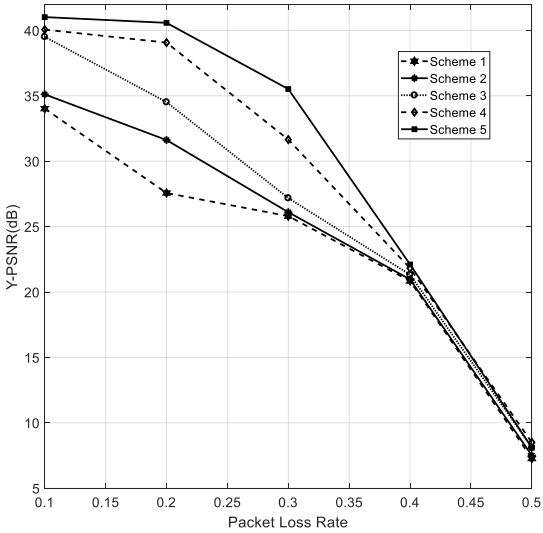

Fig. 10 – *Graph of Y-PSNR (dB) against Packet Loss Rate using SDC with GLI with the Foreman Video Sequence.*

Fig. 10 illustrates a graph of Y-PSNR (dB) against Packet Loss Rate (PLR) with a GOP length of 5 and GLI. Scheme 5 which uses GLI-SFMO exceeds Scheme 4 where ECW-FMO [11] is used by an average gain of 1.24dB. With GLI-SFMO, the inter-frame distribution of the packets causes the erroneous packets to be re-arranged in separate slices which allow the RS decoder to correct the errors. In addition, Scheme 5 which uses UEP outperforms Scheme 3 which uses EEP by an average gain of 3.33 dB in the range of $0.1 \leq PLR \leq 0.5$.

Fig. 11 illustrates the average YPSNR for each Scheme with both FLI and GLI over the packet loss rate of 0.1 to 0.5.

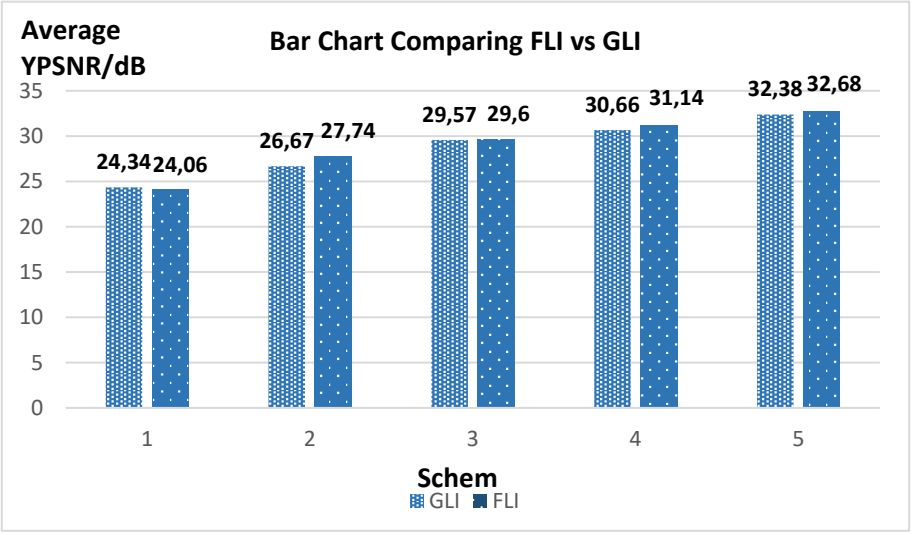

Fig. 11 – *Bar Chart representing average YPSNR/dB for Schemes 1,2,3,4 and 5.*

3.2 Using MDC with FLI Interleaving using the Gilbert Elliot Channel

Fig. 12 demonstrates a graph of Y-PSNR against Packet Loss Rate with MDC using the Gilbert Elliot Channel and FLI. Scheme 5 which uses FLI-SFMO surpasses Scheme 4 where ECW-FMO [11] is used by an average gain of 1.48 dB. In addition, Scheme 5 which uses UEP outperforms Scheme 3 which uses EEP by an average gain of 3.02 dB in the range of $0.1 \leq PLR \leq 0.5$.

Fig. 13 illustrates a graph of Y-PSNR (dB) against Packet Loss Rate (PLR) with MDC using the Gilbert Elliot Channel and GLI. It can be observed that Scheme 5 which uses GLI-SFMO exceeds Scheme 4 where ECW-FMO [11] is used by an average gain of 1.72 dB. Moreover, Scheme 5 which uses UEP outperforms Scheme 3 which uses EEP by an average gain of 2.80 dB in the range of $0.1 \leq PLR \leq 0.5$.

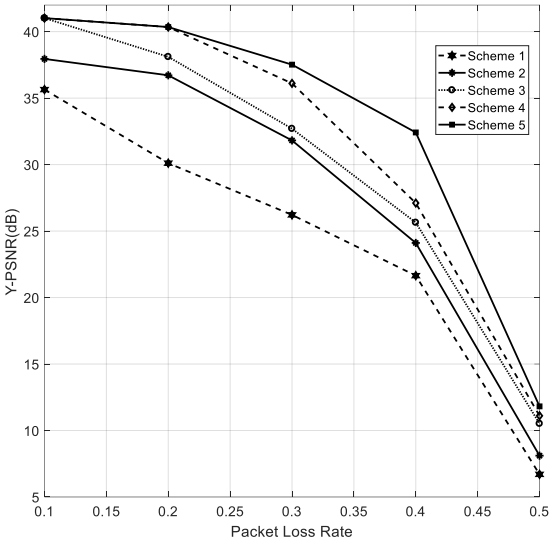

Fig. 12 – *Graph of Y-PSNR against Packet Loss Rate using MDC with the Gilbert Elliot Channel with FLI.*

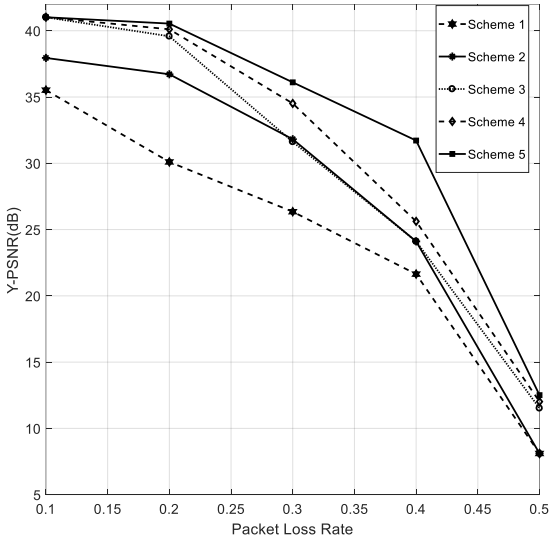

Fig. 13 – *Graph of Y-PSNR against Packet Loss Rate using MDC with the Gilbert Elliot Channel with GLI.*

The objective of MDC is to minimize the influence of noise over erroneous communication channels without the need of a retransmission. The Fig. 10 demonstrates that a higher Y-PSNR value of 31.71 dB is obtained using Scheme

5 at a PLR of 0.4 with MDC as compared to Y-PSNR value of 22.10 dB using Scheme 5 at a PLR of 0.4 with SDC from Fig. 8. Therefore, it can be observed that MDC is efficient in combatting the effect of noise leading to better results. Fig. 14 illustrates the average YPSNR for each Scheme with both FLI and GLI over the packet loss rate of 0.1 to 0.5.

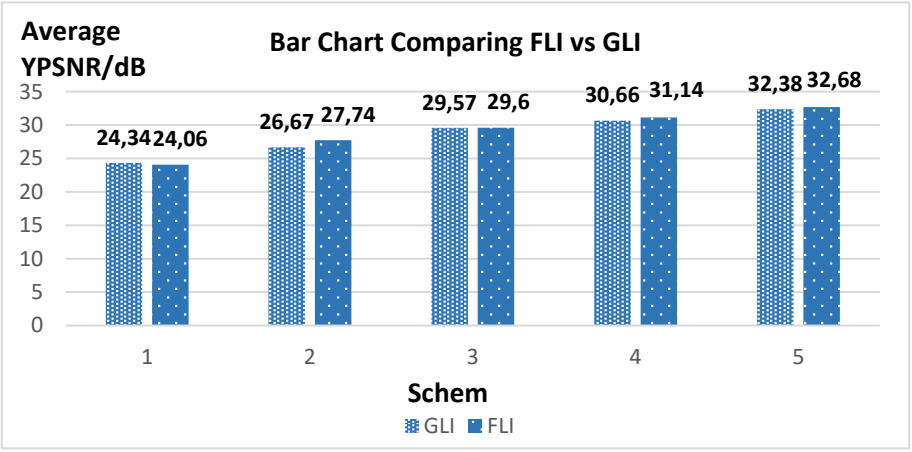

Fig. 14 – *Bar Chart representing average YPSNR/dB for Schemes 1,2,3,4 and 5.*

3.3 Using MDC with FLI Interleaving using the Composite Channel

Fig. 15 demonstrates a graph of Y-PSNR against Packet Loss Rate with MDC using the Composite Channel model and FLI. It can be seen that Scheme 5 which uses FLI-SFMO surpasses Scheme 4 where ECW-FMO [11] is used by an average gain of 0.32 dB. In addition, Scheme 5 which uses UEP outperforms Scheme 3 which uses EEP by an average gain of 0.51 dB in the range of $0.1 \leq PLR \leq 0.5$.

Fig. 16 illustrates a graph of Y-PSNR (dB) against Packet Loss Rate (PLR) with MDC using the Composite Channel model and GLI. It can be observed that Scheme 5 which uses GLI-SFMO exceeds Scheme 4 where ECW-FMO [11] is used by an average gain of 0.23 dB. In addition, Scheme 5 which uses UEP outperforms Scheme 3 which uses EEP by an average gain of 0.44 dB in the range of $0.1 \leq PLR \leq 0.5$.

Fig. 17 illustrates the average YPSNR for each Scheme with both FLI and GLI over the packet loss rate of 0.1 to 0.5.

The composite channel model, in fact, is a very powerful technique developed in [17] to efficiently model the path behavior for MDC. It can be observed from Fig. 13 that using the composite channel model, a maximum value of 41.01 dB was obtained in the range of $0.1 \leq PLR \leq 0.4$ as compared to the

Gilbert Elliot channel model where this maximum value of 41.01 dB was achievable at only a PLR value of 0.1.

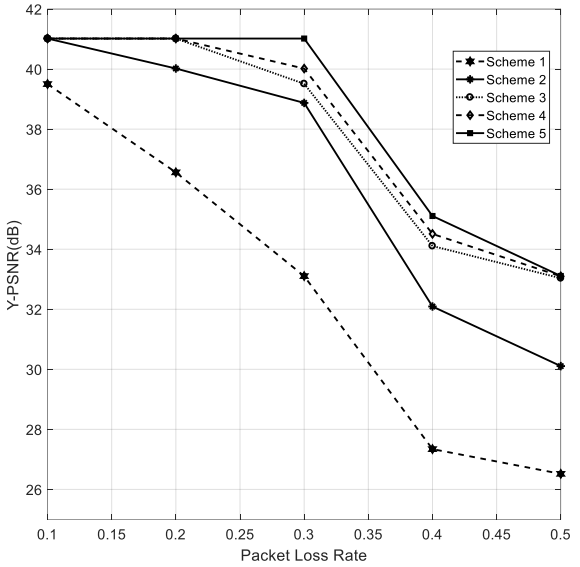

Fig. 15 – *Graph of Y-PSNR against Packet Loss Rate using MDC (Composite Channel) with FLI.*

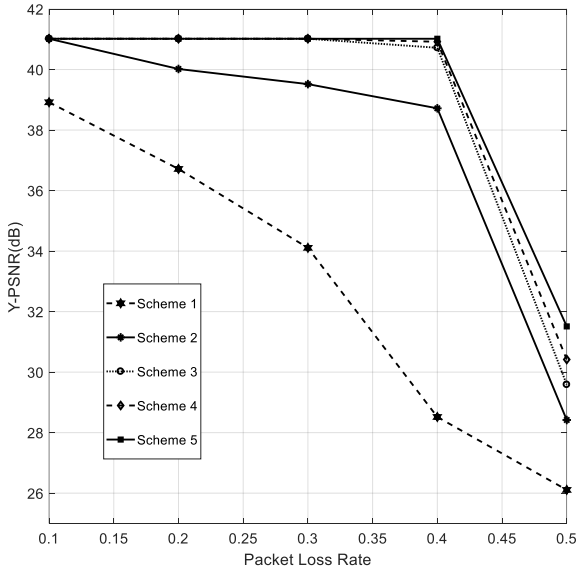

Fig. 16 – *Graph of Y-PSNR against Packet Loss Rate using MDC (Composite Channel) with GLI.*

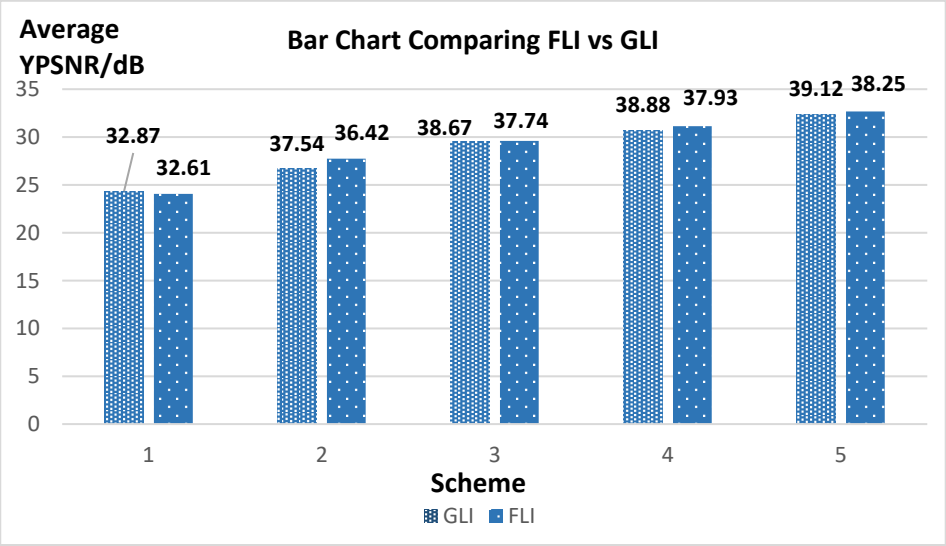

Fig. 17 – *Bar Chart representing average YPSNR/dB for Schemes 1,2,3,4 and 5.*

4 Complexity Analysis

The proposed scheme involves a minimal increase in complexity in both the encoder and decoder since it comprises of the creation of two descriptions and a new FMO scheme. **Table 4** illustrates the computations involved in the proposed framework. FLI-SMO and GLI-SFMO algorithms uses the mathematical formula to determine the new position of a MB before transmission. For a video sequence consisting of 300 frames each consisting of 99 MBs, 29700 additions, subtractions and multiplications are required for the reordering process. Nonetheless, the results have also demonstrated that significant improvements have been achieved using the proposed scheme (Scheme 5) as compared to a conventional scheme (Scheme 1). Scheme 5 uses UEP with either GLI-SFMO or FLI-SFMO whereas Scheme 1 represents the conventional scheme where EEP is used without a FMO scheme.

Table 4

Calculations involved in FLI-SFMO and GLI-SFMO.

	FLI-SFMO/GLI-SFMO Per Iteration	FLI-SFMO/GLI-SFMO Total number of Iterations (99*300)
Total number of Addition	1	29700
Total number of Subtraction	1	29700
Total number of Multiplication	1	29700

5 Conclusion

In this paper the performance of H.265 Video transmission using RS codes with UEP was further improved by introducing two new types of FMO techniques namely FLI-SFMO and GLI-SFMO. In addition, the new FMO technique was used in conjunction with MDC using the Gilbert Elliot channel model and the composite channel model to further minimize the effect of noise on the video. The proposed system has proved to be a viable solution for combatting the effect of burst errors during the transmission of compressed video over unreliable channels. A comparative analysis of the proposed system was performed by simulating five schemes using the Foreman sequence of GOP length of five. The simulation results have shown that the proposed system surpassed an EEP scheme by an average gain of 3.02 dB in the range of $0.1 \leq PLR \leq 0.5$ with FLI-SFMO. Moreover, the FLI-SFMO scheme outperformed ECW-FMO by an average gain of 1.48 dB. It was also proven that the combination of the FMO schemes with MDC was a powerful method to decrease the effect of burst errors. Therefore, the use of the proposed system could provide significant advantage to video applications in the future. Several interesting future works can be considered from this proposed technique. An interesting future work would be to test the proposed system with LDPC codes and compare its performance with RS codes. The time complexity analysis could further be evaluated along with the computational complexity. The use of machine learning techniques to reduce the computational complexity of the HEVC encoder and decoder could be also envisaged.

6 Acknowledgments

The authors are thankful to the University of Mauritius and the Higher Education Commission for providing the necessary facilities and financial support for conducting this research.

7 References

[1] Digital Technologies for a New Future, ELAC 2022, United Nations Publication, Available at: https://www.cepal.org/sites/default/files/publication/files/46817/S2000960_en.pdf

[2] Ericsson Mobility Report, 2022, Available at: https://www.ericsson.com/en/reports-and-papers/mobility-report/reports/june-2022, accessed, 15 June 2022.

[3] B. Bross, W.- J. Han, J.- R. Ohm, G. J. Sullivan, T. Wiegand: High Efficiency Video Coding (HEVC) Text Specification Draft 9, Joint Collaborative Team on Video Coding (JCT-VC) of ITU-T SG 16 WP 3 and ISO/IEC JTC 1/SC 29/WG 11, document JCTVCK1003, Shanghai, China, 2012.

[4] T. Wiegand: Draft ITU-T Recommendation and Final Draft International Standard of Joint Video Specification (ITU-T Rec. AVC |ISO/IEC 14496- 10AVC), 2003.

[5] D. Rodríguez Galiano, A. A. Del Barrio, G. Botella, D. Cuesta: Securing High-Resolution Train Videos Encoded with HEVC and Inter Prediction Mode, Computers in Industry, Vol. 121, October 2020, p. 103258.

[6] A. A. Elrowayati, M. A. Alrshah, M. F. Liew Abdullah, R. Latip: HEVC Watermarking Techniques for Authentication and Copyright Applications: Challenges and Opportunities, IEEE Access, Vol. 8, June 2020, pp. 114172 – 114189.

[7] D. J. Ringis, F. Pitié, A. Kokaram: Per Clip Lagrangian Multiplier Optimisation for HEVC, arXiv:2204.08965 [eess.IV], April 2022, p. 136

[8] R. Zhang, K. Jia, Y. Yu, P. Liu, Z. Sun: Fast 3D-HEVC Inter Coding Using Data Mining and Machine Learning, IET Image Processing, Vol. 16, No. 11, September 2022, pp. 3067 – 3084.

[9] S.- M. Tseng, C.- K. Chang, M.- Y. Liu, Y.- C. Wang: Throughput Analysis of 2-D OCDMA/Pure ALOHA Networks with Access Control and Two User Classes of Variable Length for Multimedia Traffic, Optik, Vol. 241, September 2021, p. 166928.

[10] D. Indoonundon, T. P. Fowdur, S. Soyjaudah: A Concealment Aware UEP Scheme for H.264 Using RS Codes, Indonesian Journal of Electrical Engineering and Computer Science, Vol. 6, No. 3, June 2017, pp. 671 – 681.

[11] K. Psannis, Y. Ishibashi: Efficient Flexible Macroblock Ordering Technique, IEICE Transactions on Communications, Vol. E91.B, No. 8, August 2008, pp. 2692 – 2701.

[12] J. Apostolopoulos, W. Tan, S. Wee, G. W. Wornell: Modeling Path Diversity for Multiple Description Video Communication, Proceedings of the IEEE International Conference on Acoustics, Speech, and Signal Processing, Orlando, USA, May 2002, pp. 2161 – 2164.

[13] W. El-Shafai, S. El-Rabaie, M. M. El-Halawany, F. E. Abd El-Samie: Proposed Dynamic Error Control Techniques for QoS Improvement of Wireless 3D Video Transmission, International Journal of Communication Systems, Vol. 31, No. 10, July 2018, p. e3563.

[14] Y.- C. Lin, W.- S. Wang, Y.- T. Chang: Flexible Macroblock Ordering Scramble Encryption Techniques for H.264/AVC Videos, Proceedings of Engineering and Technology Innovation, Vol. 3, August 2016, pp. 19 – 21.

[15] T. Ogunfunmi, W. C. Huang: A Flexible Macroblock Ordering with 3D MBAMAP for H.264/AVC, Proceedings of IEEE International Symposium on Circuits and Systems (ISCAS), Kobe, Japan, May 2005, pp. 3475 – 3478.

[16] D. Jurca, P. Frossard, A. Jovanovic: Forward Error Correction for Multipath Media Streaming, IEEE Transactions on Circuits and Systems for Video Technology, Vol. 19, No. 9, September 2009, pp. 1315 – 1326.

[17] T. Gao, M. Xiao, P. Chen, D. Gao: New Unequal Error Protection Strategy for Image Transmission Based on Bilayer-Lengthened PLDPC Code in Half-Duplex Relay System, Symmetry, Vol. 14, No. 8, August 2022, p. 1662.

[18] Y. Zhao, Y. Zhang, F. C. M. Lau, Z. Zhu, H. Yu: Duplicated Zigzag Decodable Fountain Codes with the Unequal Error Protection Property, Computer Communications, Vol. 185, March 2022, pp. 66 – 78.

[19] G. Ali Hussain, L. Audah: Forward Error-Correction Techniques in LTE Systems, Proceeding of the 1st International Conference on Advanced Research in Pure and Applied Science (ICARPAS), 3rd Annual Conference of Al-Muthanna University/College of Science, Al-Samawah, Iraq, March 2021, p. 050021.

[20] T. P. Fowdur, D. Indoonundon, K. M. S. Soyjaudah: A Novel Prioritised Concealment and Flexible Macroblock Ordering Scheme for Video Transmission, International Journal of Computer Applications, Vol. 150, No. 6, September 2016, pp. 35 – 42.

[21] D. Indoonundon, T. P. Fowdur, K. M. S. Soyjaudah: Enhanced H.264 Transmission with Multiple Description Coding, Prioritised Concealment and FMO, Journal of Telecommunication, Electronic and Computer Engineering, Vol. 9, No. 2, April 2017, pp. 81 – 90.